Progress in Physics of Applied Materials 6 (2026), Serial Number 10, 15 – 25

Semnan University

Progress in Physics of Applied Materials

journal homepage: https://ppam.semnan.ac.ir/

Hydrothermally Synthesized TiO_2 Nanostructures on Ti foil for Visible Light Assisted Photocatalytic Degradation of Tetracycline

Samira Yousefzadeh*, Nastaran Rostam Jadidoleslam, Kosar Moharrami

Department of Physics, Faculty of Science, Tabriz University of Technology, P.O. Box: 51335-1996, Tabriz, Iran

ARTICLE INFO

Article history:
Received: 15 June 2025
Revised: 26 July 2025
Accepted: 7 August 2025
Published online: 20 August 2025

Keywords:
TiO_2 nanostructures;
Calcination temperature;
Tetracycline;
Visible light;
Photocatalytic efficiency.

ABSTRACT

In this study, titanium dioxide (TiO_2) nanostructures on titanium foil were synthesized through a hydrothermal procedure, subsequently followed by calcination at temperatures of 500, 600, and 700 °C. The morphological, structural, and optical properties were systematically characterized using SEM, XRD, and DRS analysis. The results indicated that the calcination temperature exerts a substantial influence on the morphology and crystalline phase composition of the TiO_2 nanostructures. The calcined TiO_2 nanostructure at 600 °C (T(600)) indicated a well-defined and interconnected sheets with porous structure. This architecture enhanced the surface-to-volume ratio, light absorption and scattering, facilitated efficient charge carrier separation and improved molecular accessibility and adsorption for tetracycline (TC) degradation. The T(600) sample exhibited better performance in visible light assisted photocatalytic degradation of tetracycline as compared to T(500) and T(700) samples due to its efficient charge carrier separation and transport in a proper rutile/anatase composition. This sample reached removal efficiency of 56.50%, accompanied by a first-order kinetic rate constant of 0.0058 min^{-1} under visible light irradiation. The results were attributed visible light absorption by TC and TiO_2 nanostructures along with proper charge separation in the appropriate crystalline phase composition of the T(600) sample. These findings underscore the pivotal role of calcination temperature in optimizing TiO_2-based photocatalysts for efficient environmental remediation.

1. Introduction

Tetracycline (TC) as a type of antibiotic has been widely used in both human and veterinary medicine [1]. However, the extensive utilization of tetracycline due to major threat to public health has given rise to the development of effective degradation techniques from wastewaters and the contaminated environments [2]. In the recent years, degradation of tetracycline via photocatalytic method has garnered significant attentions. A photocatalyst uses light to expedite a photoreaction and eliminate persistent organic pollutants. Among the various photocatalytic materials, titanium dioxide (TiO_2) as a UV active semiconductor has emerged as a leading candidate due to its high chemical stability and non-toxicity [3].

The exploration of the crystal phases of TiO_2 and their influence on photocatalytic efficiency is imperative for the optimization of the design and application of TiO_2-based photocatalysts in environmental remediation [4]. The crystalline phases of the TiO_2 include brookite, anatase, and rutile phase that anatase and rutile phases play a particularly significant role in its photocatalytic efficiency. The anatase phase is known for its better photocatalytic activity compared to rutile phase, primarily due to its higher surface area and the ability to generate more reactive hydroxyl radicals (•OH) under UV light. Also, rutile phase possesses high stability, density and oxygen adsorption capacity and suffers from lower electron mobility than anatase phase [5]. Based on the reports, calcination temperature has significant and important effects on

* Corresponding author.
E-mail address: yousefzadeh@sut.ac.ir

Cite this article as:
Yousefzadeh, S., Rostam Jadidoleslam, N., and Moharrami, K., 2026. Hydrothermally Synthesized TiO_2 Nanostructures on Ti foil for Visible Light Assisted Photocatalytic Degradation of Tetracycline. *Progress in Physics of Applied Materials*, *6*(1), pp.15-25. DOI: 10.22075/ppam.2025.38104.1152

crystalline structures and the TiO_2 with mixed phase indicate higher photocatalytic degradation efficiency. However, the practical application of TiO_2 is often constrained by its substantial bandgap (approximately 3.2 eV), which restricts its activation to UV light, thereby limiting its effectiveness in utilizing the solar spectrum [6]. To address this limitation, researchers have explored various strategies to enhance the photocatalytic activity of TiO_2, including doping with metal and non-metal elements, defect engineering, coupling with other semiconductors, and the use of photosensitizers [7].

The integration of photosensitizers into TiO_2-based photocatalytic systems has been demonstrated to be a successful strategy to improve visible light absorption and overall photocatalytic performance. Tetracycline itself has the capacity as a photosensitizer due to its propensity in visible light absorption. This dual role of tetracycline not only facilitates its degradation but also opens new avenues for the development of advanced photocatalytic systems that can effectively address the challenges posed by antibiotic pollution in the environment [8]. Most of researches investigated the photocatalytic degradation of tetracycline over TiO_2 under UV light [9-11] and there are few reports on the sensitization of the TiO_2 by antibiotics and its photocatalytic activity in visible range. For instance, TiO_2-P25 achieved 25.1% TC removal under 700 nm light and mineralized 35.7% of TC under UV light (350 nm) [12]. Furthermore, Qin and co-workers showed the effective visible light photocatalytic degradation of TC by the sensitized pure TiO_2 via a ligand-to-metal charge transfer mechanism [13].

On the other hand, one of the challenges in (photo)catalytic activity is the separation of photocatalyst materials after photodegradation. In this regard, deposition of photoactive materials on suitable substrate can solve the separation and collection of them from pollutants solutions. For example, Ti^{3+} and N-codoped TiO_2 nanotube array on titanium foil exhibit excellent electrochemical degradation performance (100%) of tetracycline and metronidazole within 240 min [14].

In this study, the photocatalytic degradation of tetracycline under visible light irradiation was investigated using TiO_2 nanostructures on titanium (Ti) foil. This research focuses on the structural, morphological, optical, and photocatalytic properties of the synthesized TiO_2 nanostructures on Ti foil at different calcination temperatures. Furthermore, visible light photodegradation of TC over the TiO_2 nanostructures and the effect of different parameters on photocatalytic activity were studied.

Also, to our knowledge, this is the first report on visible light photocatalytic degradation of TC by the TiO_2 nanostructures on substrate, calcined at different temperatures. Calcination temperatures influence on the crystalline structures and electron-hole separation and transfer in visible light activated photocatalytic degradation of TC. Due to deposition of the TiO_2 on the Ti foil, the photocatalysts can easily be separated and recovered from wastewater. Photodegradation of the TC under visible light of the LED is one of other benefits of this work.

2. Materials and methods

2.1. Chemicals

Titanium foil (Grade 2, thickness: 0.5 mm) and isopropyl alcohol were purchased from Loterios and Mojallali company, respectively. Hydrochloric acid (HCl) was provided from Merck. Ammonium oxalate, sodium hydroxide (NaOH), and ascorbic acid were prepared from Sigma-Aldrich.

2.2. Fabrication of TiO_2 nanostructures on Ti foil

After polishing with sandpaper, a Ti foil (30×20 mm^2) was cleaned in a mixture of water, acetone, and isopropanol (volume ratio: 1:1:1) by ultrasonication for 30 min. Then, it was placed at a specific angle in a (25 mL) Teflon lined hydrothermal autoclave, containing 20 mL of 1 M NaOH solution. Subsequently, the autoclave was attained at temperature of 200 °C for 24 h. Then, the autoclave was cooled down and the Ti foil was removed. The Ti foil was immersed in 30 mL of 0.6 M HCl solution for 1 h to facilitate the exchange of Na^+ ions with H^+ ions. The Ti foil was thoroughly washed with deionized water and dried at room temperature. The obtained layer was calcined at different temperatures (500, 600, and 700 °C) for 2 h and named as T(500), T(600), and T(700), respectively [15].

2.3. Characterization

The morphology and surface characteristics of the fabricated TiO_2 nanostructures were analyzed using a scanning electron microscope (SEM, QUANTA-200), equipped with Energy-dispersive X-ray spectroscopy (EDS) elemental mapping. The crystalline structure of the samples was examined via X-ray diffraction (XRD) (Bruker, D8-Advance). The optical properties of the synthesized samples were studied using diffuse reflectance spectroscopy (DRS, Evolution-220).

2.4. Photocatalytic degradation

Photocatalytic degradation of the TC was performed using TiO_2 samples in a photochemical reactor. A white LED lamp (50 W) provided by Anashid Gostar Novin Iranian Co., served as the visible light source and located at distance of 5 cm from the sample. The calcined TiO_2 at different temperatures was placed on a Teflon stand in 40 mL of TC solution and the solution was stirred under dark condition for 30 min for adsorption-desorption equilibrium. Then, to evaluate the degradation of tetracycline (TC) under visible light irradiation, 2.5 mL of the solution was removed at 15 min time intervals and TC concentration was evaluated by UV-visible absorption spectroscopy. Based on the Beer-Lambert's law and relation between TC concentration and optical absorption, photocatalytic degradation efficiency (η) was calculated by:

$$\eta=(1-(C_t/C_0)) \times 100 \quad (1)$$

where C_0 is initial TC concentration and C_t is TC concentration at each time interval. All experiments were

conducted at room temperature. The effect of TC concentration on photodegradation efficiency was analyzed at different initial concentrations of TC (5, 10, and 15 mg/L). The stability and reusability of the TiO_2 photocatalysts were performed over multiple cycles of degradation experiments. To identify the dominant reactive species in the photocatalytic process, ascorbic acid (AA), isopropanol (IPA), and ammonium oxalate (AO) were used as superoxide radical, hydroxyl radical, and hole scavenger, respectively.

3. Results and Discussion

The morphological evolution of the calcined samples at different temperatures (500, 600, and 700 °C) was systematically examined through scanning electron microscopy (SEM) (Fig. 1). At temperature of 500 °C (Fig. 1(a)), the surface demonstrated a relatively dense architecture, composed of the entangled nanowires. A noticeable degree of nanowire agglomeration entanglement was observed, leading to a poorly developed porous network and a restricted surface area [16, 17], thereby limiting the potential for photocatalytic reactions. Figure 1(b) shows SEM image of the calcined TiO_2 at 600 °C that a substantial enhancement in morphology was observed, accompanied by the emergence of a well-defined and interconnected sheets with porous structure. This architecture not only enhanced the surface area but also improved molecular accessibility and adsorption of tetracycline, promoted light absorption and scattering and facilitated efficient charge carrier separation in photocatalytic activity [18-20].

At temperature of 700 °C Figure 1(c), an excessive grain and particle growth were evident and lead to a substantial reduction in porosity and surface area. This morphology compromises the structural characteristics necessary for effective photocatalyst [21, 22]. These observations indicate that calcination at 600 °C yields the most favorable morphological attributes for photocatalytic applications. The optimized pore structure, augmented specific surface area, enhanced crystallinity, and superior photophysical properties at this temperature synergistically improve the degradation efficiency of tetracycline [23-25]. These results underscore that 600 °C is the critical temperature for engineering titanium oxide nanostructures with high photocatalytic performance. It is hypothesized that these morphological features will have a significant impact on the photocatalytic behavior of the samples. The photocatalytic degradation performance of the synthesized TiO_2 under visible light irradiation is provided in the subsequent sections.

EDS elemental mapping was conducted to investigate the distribution of titanium (Ti) and oxygen (O) within all samples Figure 2. The EDS maps demonstrated a homogeneous distribution of both Ti and O across the examined area of all samples. The uniform distribution of titanium and oxygen indicates the formation of a well-organized titanium dioxide (TiO_2).

Based on the results of the XRD analysis (Fig. 3) for the synthesized TiO_2 at different temperatures, the structural and phase changes in the samples are clearly observable. At 500 °C, the XRD pattern exhibits characteristic peaks corresponding to the anatase phase of the TiO_2 (Fig. 3(a)). The main anatase peaks appear at 2θ=25.3, 37.8, and 48.0°, related to (101), (004), and (200) crystal planes, respectively. These results indicate that the crystalline structure of the sample at this temperature is predominantly anatase, with a moderate degree of crystallinity. Notably, a minor fraction of the rutile phase is also present, as evidenced by the emergence of a weak peak at 2θ=27.4°, attributed to (110) plane [26], suggesting the initial stages of phase transformation. The peaks marked with an asterisk (*) correspond to Ti, resulted from the titanium substrate. The diffraction patterns for the sample calcined at 600 °C (Fig. 3(b)) show significant improvements in peak intensity and clarity, indicating a change in crystallinity and structural order [27]. At this temperature, the anatase phase remains predominant. However, peaks corresponding to the rutile phase become more pronounced at 27.4, 36.1, and 54.3° from (110), (101), and (210) planes, respectively [26, 27]. These results signify a progressive phase transition from anatase to rutile. The presence of these peaks exhibits that while anatase remains the dominant phase, the proportion of rutile has significantly increased compared to 500 °C. The XRD pattern for the synthesized samples at 700 °C in Figure 3(c) demonstrate substantial alterations, with rutile becoming the predominant phase. The main rutile peaks dominate the pattern, while the intensity of anatase peaks is significantly reduced. Although traces of anatase can still be observed, its fraction is considerably lower than the other temperatures. These results confirm that the anatase-to-rutile phase transformation continues at this temperature, leading to the formation of a primarily rutile-structured TiO_2 sample [28]. The phase composition analysis reveals that at 500 °C, the sample consists of 87% anatase and 11% rutile, indicating the onset of the phase transition. At 600 °C, the rutile content increases to approximately 23%, reflecting a substantial progression in the transformation. Finally, at 700 °C, the rutile phase dominates, comprising 49% of the crystalline structure, with only 22% anatase remaining. These findings highlight the temperature-dependent phase evolution of the TiO_2, where the anatase to rutile transformation initiates at 500 °C [15, 29]. The crystallite sizes of the TiO_2 samples calcined at different temperatures were estimated using the Debye–Scherrer equation [3]:

$$D=K\lambda/\beta\cos\theta \quad (2)$$

where D is the crystalline size, K is the shape factor, λ is the X-ray wavelength (0.15406 nm for Cu Kα radiation), β is the full width at half maximum (FWHM) of the diffraction peak, and θ is the Bragg angle. The (101) diffraction peak, located around $2\theta \approx 25.3°$, was used for these calculations.

The crystalline sizes were obtained at about 33.17, 31.92, and 26.57 nm for T(500), T(600), and T(700) samples, respectively. By increasing the calcination temperature crystalline size decreases and this trend suggests that higher calcination temperatures may promote structural rearrangements or phase transformations.

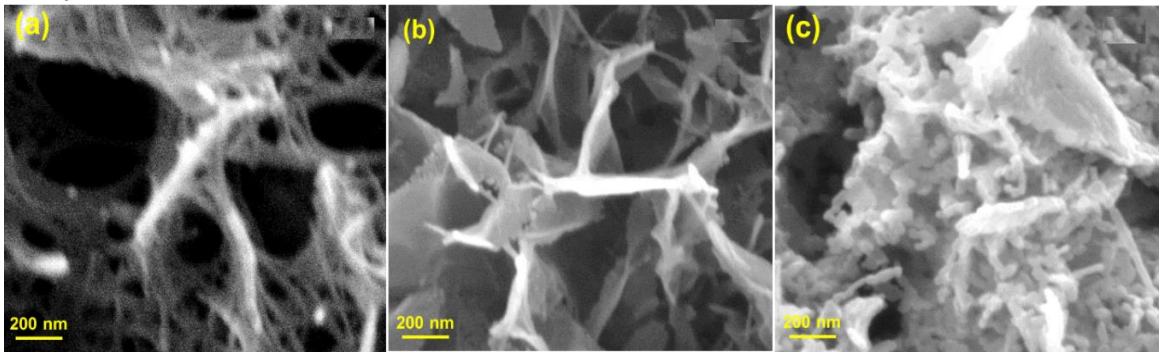

Fig. 1. SEM images of the calcined TiO_2 at temperature of (a) 500, (b) 600, and (c) 700 °C.

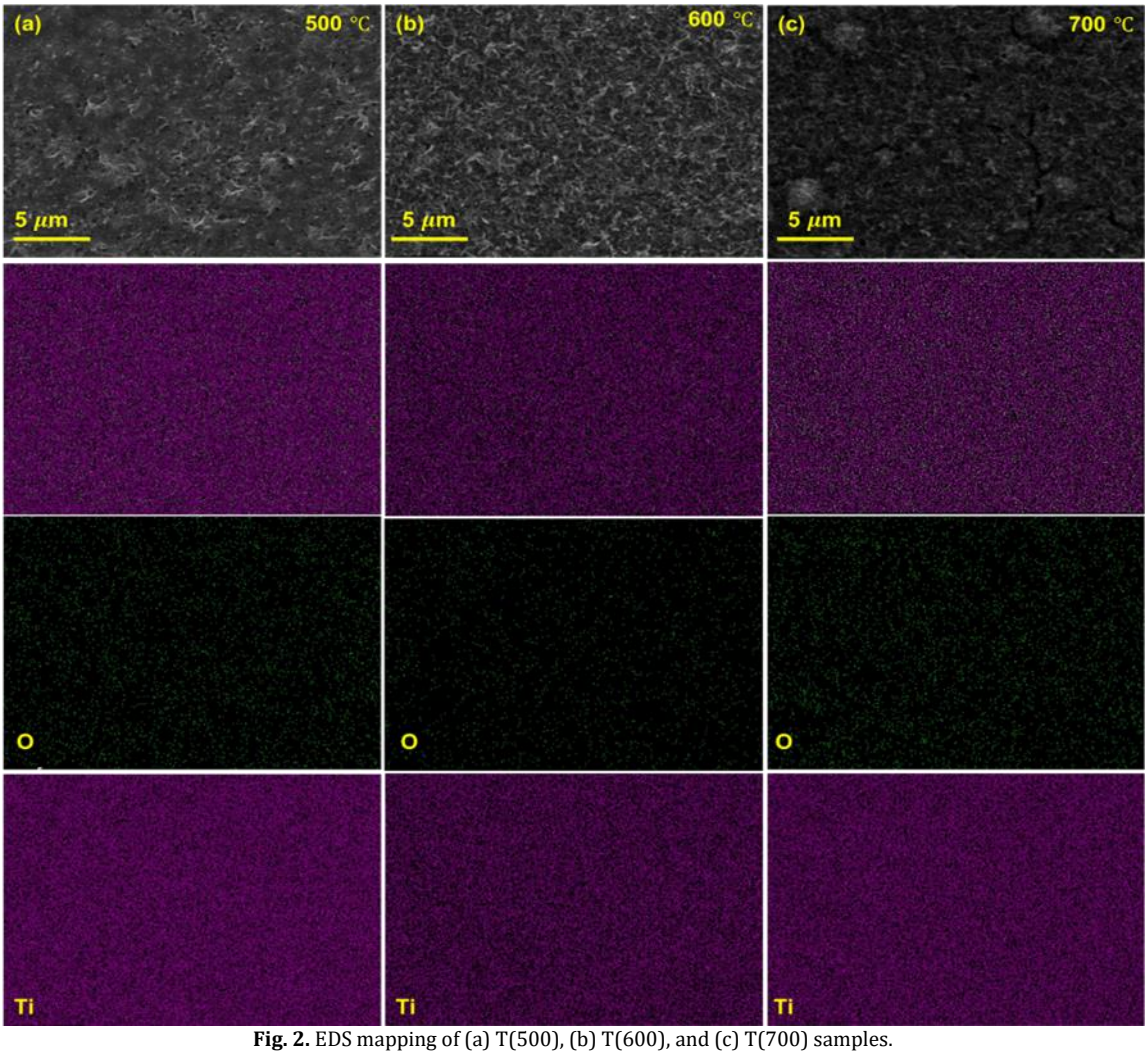

Fig. 2. EDS mapping of (a) T(500), (b) T(600), and (c) T(700) samples.

In this study, the optical properties of the TiO_2 nanostructures, calcined at different temperatures were investigated using diffuse reflectance spectroscopy. The results demonstrated that increasing the synthesis temperature did not lead to a noticeable shift in the absorption edge, as depicted in Figure 4(a). The absorption edge for all samples was found to be approximately 385 nm [30, 31]. Light absorption of the TiO_2 samples in visible region is resulted from light scattering in TiO_2 nanostructures, oxygen vacancies and Ti^{+3} species. The oxygen vacancies, and Ti^{+3} species create defect energy level below the conduction band (CB). Under visible light irradiation, and by absorbing visible light, the excited electrons transformed from Ti^{+3} state to conduction band of TiO_2 [32-34]. Tauc plot analysis revealed the band gap energy for different samples, as shown in Figure 4(b). The

band gap energies for the fabricated samples at temperatures of 500, 600, and 700 °C was calculated at about 3.1, 3.2, and 3.3 eV, respectively [31, 35].

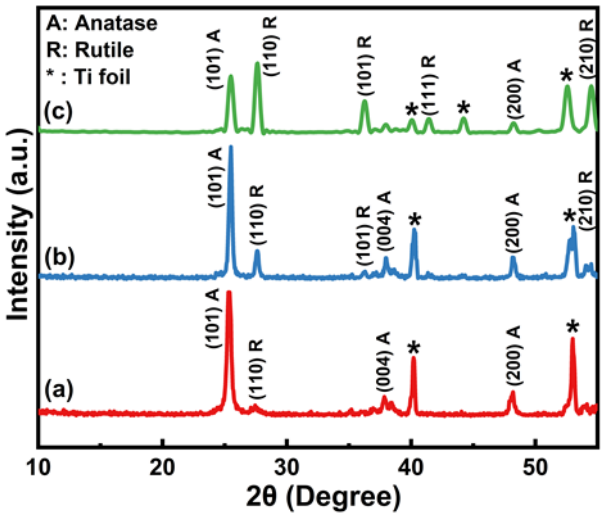

Fig. 3. XRD patterns of (a) T(500) , (b) T(600), and (c) T(700) samples.

The photocatalytic degradation of tetracycline over the synthesized TiO_2 nanostructures was investigated under white LED light irradiation for 40 mL of the TC solution (10 mg/L). As shown in Figure 5(a), in the absence of the TiO_2 samples, the concentration ratio (C_t/C_0) exhibited change within 120 min, indicating low photolysis of the TC. The adsorption process reached equilibrium within this period, with approximately 10.0%, 8.9%, and 5.8% of TC removed for T(500), T(600), and T(700), respectively. This finding highlights the significant role of TiO_2's surface interactions, which contribute to the overall removal efficiency even before light irradiation [36, 37]. The adsorption capacity is likely influenced by the surface area and active sites of TiO_2, facilitating electrostatic interactions and hydrogen bonding with TC molecules [38]. In the present study, the effect of visible light irradiation on the degradation of the tetracycline for different samples was studied, as shown in Figure 5(b). The removal efficiencies of the TC were achieved at about 40.60, 56.50, and 31.98% for the T(500), T(600), and T(700) within 120 min, respectively. The degradation efficiencies followed the order: T(600)>T(500)>T(700), highlighting the significant impact of calcination temperature on the catalytic performance. The optimal activity of the sample synthesized at 600 °C is attributed to its favorable phase composition, crystallinity, and surface properties, which enhance light absorption and charge separation and minimize recombination effects [23]. In contrast, the reduced performance of the T(700) sample is likely due to particle aggregation, decreased surface area, and potential phase transitions, which might lead to the formation of a less active TiO_2 phase (such as rutile) [19]. The photocatalytic degradation kinetics of tetracycline was expressed with the following equation [38, 39]:

$$Ln(C_0/C_t) = kt \quad (3)$$

where k is the first-order rate constant and t is the reaction time. All experiments were conducted at room temperature. Kinetic analysis revealed that the photocatalytic degradation of tetracycline follows first-order kinetics. The high degree of agreement of the data with the linear relationship (regression coefficients, R^2= 0.98, 0.99, and 0.96 for the T(500), T(600), and T(700) samples, respectively) suggests compatibility with the Langmuir-Hinshelwood model, which describes the photocatalytic reaction mechanism [38, 40]. As demonstrated in Figure 5(c) and (d), kinetic analysis based on the $\ln(C_0/C_t)$ vs t plot indicated that the TiO_2 sample calcined at 600 °C exhibited the optimal performance, achieving a degradation efficiency of 56.50% and a kinetic constant of k= 0.0058 min^{-1}.

The T(500) showed a degradation efficiency of 40.60%, with a kinetic constant of k= 0.0041 min^{-1}, while the T(700) indicated a lower efficiency of 31.98% and kinetic constant of k= 0.0028 min^{-1}. At higher calcination temperatures, such as 700 °C, the aggregated structure leads to a decrease in the overall surface area available for photocatalytic reactions, which negatively affects the degradation efficiency [41].

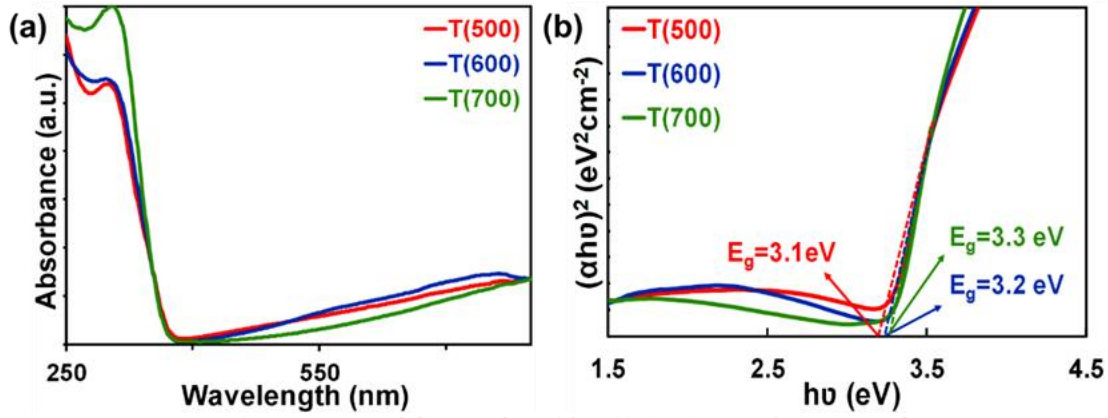

Fig. 4. (a) DRS spectra and (b) Tauc plots of the T(500), T(600), and T(700) samples.

In addition, phase transitions at temperature of 700 °C result in a shift from the anatase phase to rutile, a phase that has lower photocatalytic activity due to less efficient charge carrier dynamics [42]. These findings underscore

the importance of optimizing the calcination temperature to maximize the photocatalytic efficiency of TiO_2 for the degradation of organic pollutants under visible light irradiation [41, 42]. Table 1 compares the photocatalytic results of the TiO_2 nanostructures in this work.

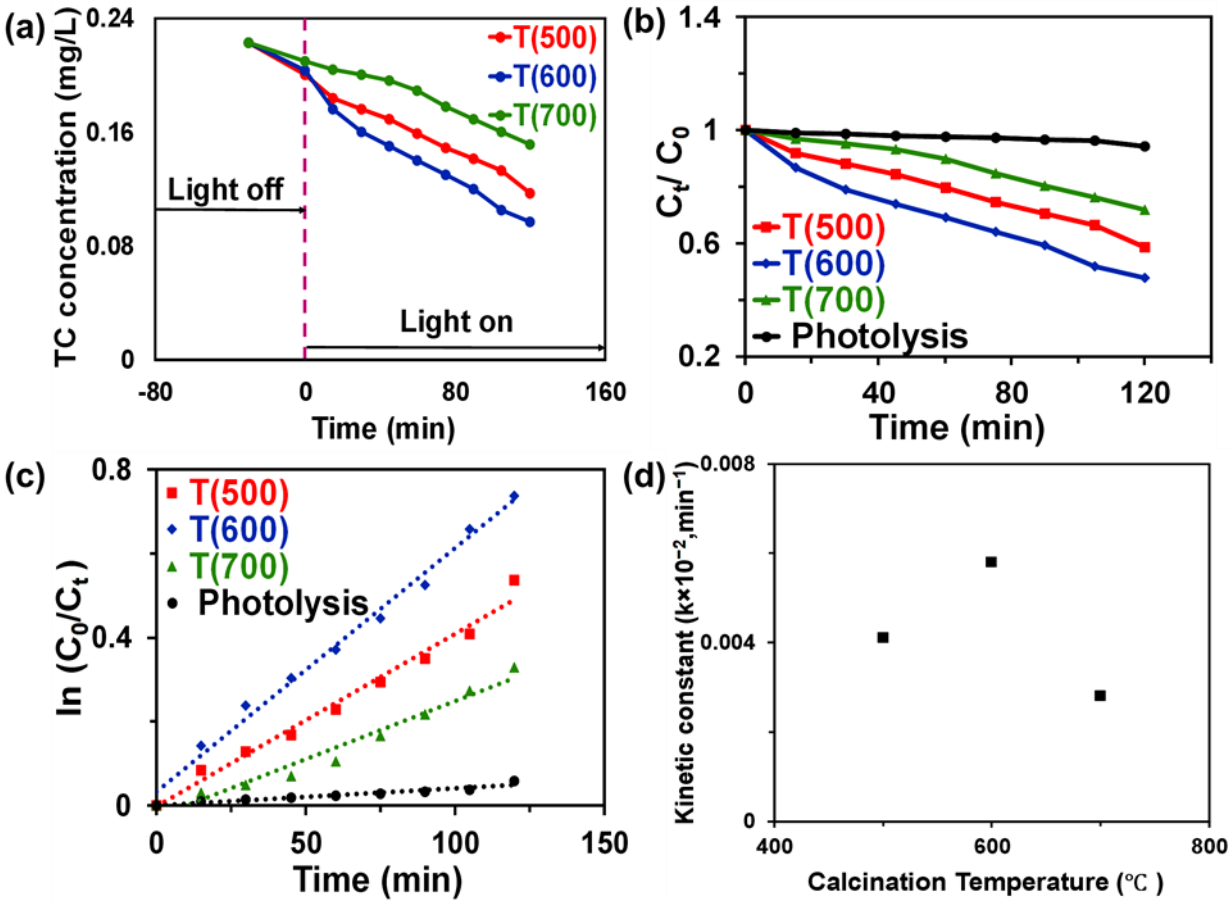

Fig. 5. (a, b) Photodegradation of TC (under visible light irradiation, with an initial TC concentration of 10 mg/L), (c) $Ln(C_0/C_t)$-t plot of the T(500), T(600), and T(700) samples, and (d) Kinetic constants of the TiO_2 samples as a function of calcination temperature.

Table 1. Comparison of the TiO_2 samples in photocatalytic degradation of TC.

Sample	Calcination temperature (°C)	Degradation efficiency (%)	Rate constant (min^{-1})
T(500)	500	40.60	0.0041
T(600)	600	56.50	0.0058
T(700)	700	31.98	0.0028

The effect of the initial concentration of tetracycline on the photocatalytic degradation efficiency using the T(600) is shown in Figure 6(a). The temporal changes in tetracycline concentration at three distinct initial concentrations (5, 10, and 15 mg/L) over a duration of 120 min are investigated. The results imply a consistent decrease for all concentrations, thereby indicating the gradual degradation of the compound under the prevailing experimental conditions. The degradation efficiency strongly depends on the initial pollutant concentration [43]. The photocatalytic efficiency reached 56.50% at an initial concentration of 10 mg/L. When the initial concentration was 5 mg/L, the degradation was about 33.06%, indicating lower photodegradation efficiency than concentration of 10 mg/L. At 15 mg/L, the degradation was only 25% and indicated that the process slowed down at higher concentrations [44].

This decrease in degradation performance at higher concentrations can be attributed to several known factors: (i) The higher numbers of tetracycline molecules in the solution leads to decreased light absorption and scattering, which reduces the intensity of photons reaching the photocatalyst surface and limits the generation of electron-hole pairs [45]; (ii) At higher concentrations, salt layers or organic films are formed on surface of the catalyst, impeding the transport of reactive species (e.g., hydroxyl radicals) and inhibiting the overall catalytic process [46]; (iii) The accumulation of degradation intermediates

(including dehydrated tetracycline derivatives and nitrogen-containing compounds) at high concentration can block catalytic sites or interfere with key degradation pathways, further reducing the efficiency of the system [47]. Certain limitations associated with lower concentration can be recognized: (i) lower concentration of tetracycline molecules reduce effective interactions between TC and reactive species, which can affect the overall degradation rate [48]; (ii) under low concentration condition, side reactions (such as water or background ion oxidation) may dominate, leading to inefficient utilization of photogenerated reactive species [3]; (iii) at lower initial concentration, the small absolute change in TC levels over time can complicate kinetic assessments and make it difficult to capture meaningful removal trends [45].

The results of the photocatalytic stability and reusability of the T(600) photocatalyst were evaluated through three consecutive cycles of tetracycline degradation (10 mg/L). Figure 6(b) demonstrated considerable stability with degradation efficiencies reported as 56.50%, 55.24%, and 46.95% for the first, second, and third cycles, respectively. The average degradation efficiency over these three cycles was 52.7%, indicating only a slight reduction of 5% from the first to the third cycle. A slight decrease in catalytic activity may occur due to the partial loss during the recovery process and possibly the accumulation of intermediate by-products on the catalyst surface [49, 50]. However, the results of this study showed that the synthesized TiO_2 photocatalysts through a hydrothermal method demonstrates significant stability. It is capable of maintaining its effective performance for the degradation of tetracycline in aqueous solutions across multiple cycles. This attribute makes it suitable for practical applications in water and wastewater treatment processes. Moreover, separation of the synthesized photocatalyst materials after photodegradation was easily performed.

To identify the active species involved in the photocatalytic degradation of TC on the T(600) sample under visible light irradiation, three scavengers AA, IPA, and AO were employed to deactivate superoxide radical ($^{\bullet}O_2^-$), hydroxyl radical ($^{\bullet}OH$), and hole (h^+), respectively [51, 52]. As shown in Figure 7, the addition of ascorbic acid (AA) decreased the degradation efficiency of TC from 56.50% to 29.53%, indicating the role of $^{\bullet}O_2^-$. When AO was introduced, the efficiency reduced to 36.05%, demonstrating the contribution of h^+. Similarly, the presence of IPA lowered the removal efficiency to 41.35%, confirming the involvement of $^{\bullet}OH$. These results suggest that active species of the $^{\bullet}O_2^-$, h^+, and $^{\bullet}OH$ play roles in the photocatalytic degradation of TC on TiO_2 under visible light irradiation, aligning with previous observations [48, 52].

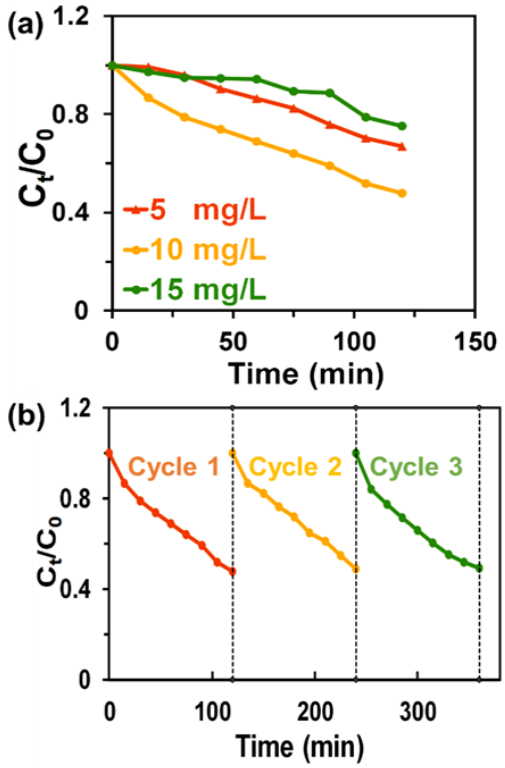

Fig. 6. (a) The effect of tetracycline concentration on photodegradation efficiency and (b) stability of the T(600) sample.

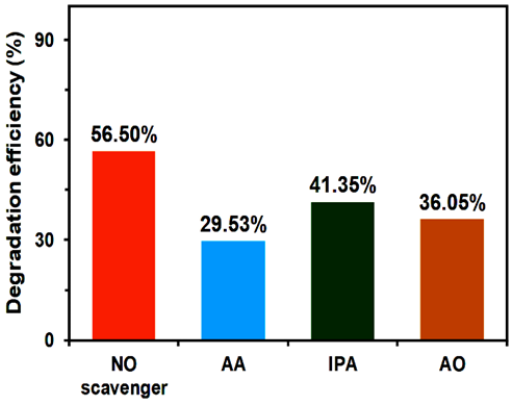

Fig. 7. Effect of different scavengers on TC photodegradation over T(600) (under visible light irradiation, Initial TC concentration: 10 mg/L).

Based on our results, photodegradation of TC under visible light can proceed by two ways. (Fig. 8) shows the schematics of the proposed mechanisms. The creation of oxygen vacancies (Ov) and Ti^{3+} species during the synthesis and calcination processes leads to the formation of mid-gap states within the TiO_2 band structure [53, 54]. These structural defects play a critical role in enhancing photocatalytic performance under visible light irradiation, primarily through two mechanisms: (i) extension of light absorption into the visible region and (ii) reduction of electron-hole recombination [53, 55].

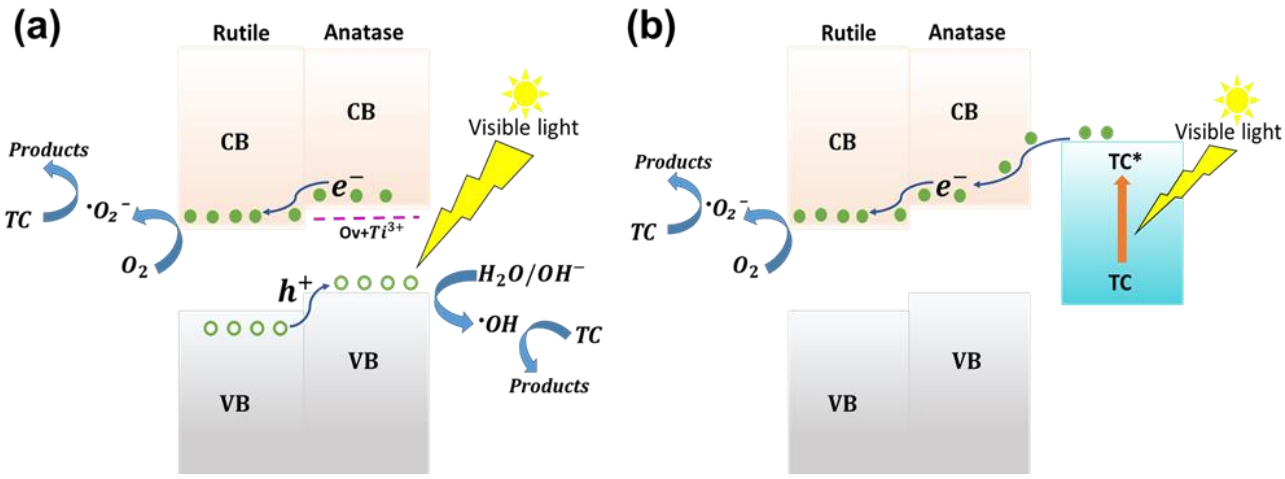

Fig. 1. (a) and (b)The proposed mechanisms of TC photodegradation under visible light.

Upon visible light irradiation, electrons can be transferred to the CB from the defect states associated with Ti^{3+} species. The corresponding reaction for this process is as follows [53]:

$$TiO_2 + h\upsilon \rightarrow e^- + h^+ \quad (4)$$

Defect states act as electron traps, capturing the excited electrons and thereby reducing the direct recombination of electron-hole pairs [54, 55]. This phenomenon increases the carrier lifetime and facilitates oxidation-reduction reactions on the TiO_2 surface. In the anatase–rutile heterojunction of the synthesized TiO_2 nanostructures, the two phases form a type-II band alignment, where the conduction band minimum of rutile is slightly lower than that of anatase, while the valence band (VB) maximum of anatase is higher than that of rutile [56]. As a result, the photogenerated electrons preferentially transfer from CB of the anatase phase to CB of the rutile phase. This band structure effectively separates photogenerated electrons. Electrons transfer to CB of the rutile and subsequently react with dissolved oxygen molecules to generate superoxide radicals ($\cdot O_2^-$):

$$e^- + O_2 \rightarrow \cdot O_2^- \quad (5)$$

Meanwhile, the holes produced in the VB transferred in the opposite direction and can react with water molecules or surface-adsorbed hydroxyl ions to generate hydroxyl radicals ($\cdot$OH):

$$h^+ + H_2O \rightarrow \cdot OH + H^+ \quad (6)$$

$$h^+ + OH^- \rightarrow \cdot OH \quad (7)$$

The generated $\cdot O_2^-$ and $\cdot$OH radicals, along with the oxidative power of the holes (h^+), attacked tetracycline (TC), breaking them down into harmless mineral products [55]:

$$TC + (\cdot O_2^-, \cdot OH, h^+) \rightarrow Products \quad (8)$$

Therefore, the synergistic effect of visible light absorption by the defect states and enhanced charge separation significantly improves the photocatalytic degradation efficiency of defect-rich TiO_2 Figure 8(a). On the other hand, upon visible-light irradiation, the adsorbed tetracycline (TC) molecules on surface of the TiO_2 nanostructures act as sensitizers. Therefore, the TC molecules absorb visible light photons due to their intrinsic electronic structure and are excited from the ground state to an excited state (TC*). The excited TC* species can inject electrons into the conduction band (CB) of TiO_2 [12, 13]. This electron injection is facilitated by the suitable alignment of energy levels between the excited state of TC and the CB of the TiO_2 nanostructures (combination of rutile and anatase phase). The transferred electrons produced the superoxide radicals as active species for TC Figure 8(b). As shown in SEM image, the calcined TiO_2 at 600 °C indicated a well-defined and interconnected sheets with porous structure. This architecture enhanced the surface-to-volume ratio, light absorption and scattering, facilitated efficient charge carrier separation and improved molecular accessibility and adsorption for tetracycline degradation. Also, XRD pattern of the TiO_2 nanostructures exhibited that a proper rutile content relative to anatase was formed at calcination temperature of 600 °C.

4. Conclusions

In summary, the present study underscores the effect of calcination temperatures on the photocatalytic efficiency of the TiO_2 nanostructures on Ti foil for the degradation of tetracycline under visible light. The results indicate that the synthesized TiO_2 nanostructure at temperature of 600 °C exhibits higher performance in comparison to the others, with notable stability and reusability. The T(600) showed a well-defined and interconnected sheets with porous structure. This architecture enhanced the surface area, light absorption, improved molecular accessibility and adsorption for tetracycline degradation. Also, efficient charge carrier separation and transport was supplied by a proper rutile/anatase composition in the T(600) sample.

Acknowledgements

This research was supported by Research and Technology Council of Sahand University of Technology.

Funding Statement

This research received no specific grant from any funding agency.

Conflicts of interest

The authors declare that they have no known competing financial interests or personal relationships that could have appeared to influence the work reported in this paper.

Authors contribution statement

Samira Yousefzadeh: Conceptualization, Methodology, Software, Formal analysis, Investigation, Resources, Data Curation, Validation, Visualization, Supervision, Funding acquisition, Writing - Original Draft, Writing - Review & Editing;
Nastaran Rostam Jadidoleslam: Methodology, Software, Formal analysis, Resources, Writing - Original Draft, Writing - Review & Editing;
Kosar Moharrami: Methodology, Formal analysis, Resources, Investigation

References

[1] Kounatidis, D., Dalamaga, M., Grivakou, E., Karampela, I., Koufopoulos, P., Dalopoulos, V., Adamidis, N., Mylona, E., Kaziani, A. and Vallianou, N.G., 2024. Third-generation tetracyclines: current knowledge and therapeutic potential. *Biomolecules*, *14*(7), p.783.

[2] Daghrir, R. and Drogui, P., 2013. Tetracycline antibiotics in the environment: a review. *Environmental chemistry letters*, *11*(3), pp.209-227.

[3] Zenou, V.Y. and Bakardjieva, S., 2018. Microstructural analysis of undoped and moderately Sc-doped TiO_2 anatase nanoparticles using Scherrer equation and Debye function analysis. *Materials Characterization*, *144*, pp.287-296.

[4] Ma, J., Chen, Y., Zhou, G., Ge, H. and Liu, H., 2024. Recent advances in photocatalytic degradation of tetracycline antibiotics. *Catalysts*, *14*(11), p.762.

[5] Chiarello, G.L., Paola, A.D., Palmisano, L. and Selli, E., 2011. Effect of titanium dioxide crystalline structure on the photocatalytic production of hydrogen. *Photochemical & Photobiological Sciences*, *10*(3), pp.355-360.

[6] Filippatos, P.P., Kelaidis, N., Vasilopoulou, M., Davazoglou, D. and Chroneos, A., 2021. Structural, electronic, and optical properties of group 6 doped anatase TiO2: a theoretical approach. *Applied Sciences*, *11*(4), p.1657.

[7] Peiris, S., de Silva, H.B., Ranasinghe, K.N., Bandara, S.V. and Perera, I.R., 2021. Recent development and future prospects of TiO_2 photocatalysis. *Journal of the Chinese Chemical Society*, 68(5), pp.738-769.

[8] Hamza, M.A., Abd El-Rahman, S.A., Ramadan, S.K., Ezz-Elregal, E.-E.M., Rizk, S.A. and Abou-Gamra, Z.M., 2024. The enhanced visible-light-driven photocatalytic performance of nanocrystalline TiO_2 decorated by quinazolinone-photosensitizer toward photocatalytic treatment of simulated wastewater. *Journal of Photochemistry and Photobiology A: Chemistry*, 452, p.115599.

[9] Qu, J., Chen, D., Li, N., Xu, Q., Li, H., He, J. and Lu, J., 2019. Ternary photocatalyst of atomic-scale Pt coupled with MoS_2 co-loaded on TiO_2 surface for highly efficient degradation of gaseous toluene. *Applied Catalysis B: Environmental*, 256, p.117877.

[10] Reyes, C., Fernandez, J., Freer, J., Mondaca, M.A., Zaror, C., Malato, S. and Mansilla, H.D., 2006. Degradation and inactivation of tetracycline by TiO_2 photocatalysis. *Journal of Photochemistry and Photobiology A: Chemistry*, *184*(1-2), pp.141-146.

[11] Zhu, X.D., Wang, Y.J., Sun, R.J. and Zhou, D.M., 2013. Photocatalytic degradation of tetracycline in aqueous solution by nanosized TiO_2. *Chemosphere*, 92(8), pp.925-932.

[12] Wu, S., Hu, H., Lin, Y., Zhang, J. and Hu, Y.H., 2020. Visible light photocatalytic degradation of tetracycline over TiO_2. *Chemical Engineering Journal*, 382, p.122842.

[13] Qin, C., Tang, J., Qiao, R. and Lin, S., 2022. Tetracycline sensitizes TiO_2 for visible light photocatalytic degradation via ligand-to-metal charge transfer. *Chinese Chemical Letters*, 33(12), pp.5218-5222.

[14] Pang, D., Liu, Y., Song, H., Chen, D., Zhu, W., Liu, R., Yang, H., Li, A. and Zhang, S., 2021. Trace Ti^{3+}-and N-codoped TiO_2 nanotube array anode for significantly enhanced electrocatalytic degradation of tetracycline and metronidazole. *Chemical Engineering Journal*, 405, p.126982.

[15] Liu, B., Deng, D., Lee, J.Y. and Aydil, E.S., 2010. Oriented single-crystalline TiO_2 nanowires on titanium foil for lithium ion batteries. *Journal of Materials Research*, 25(8), pp.1588-1594.

[16] Peng, L., Xu, X., Lv, Z., Song, J., He, M., Wang, Q., Yan, L., Li, Y. and Li, Z., 2012. Thermal and morphological study of Al_2O_3 nanofibers derived from boehmite precursor. *Journal of thermal analysis and calorimetry*, 110(2), pp.749-754.

[17] Hasmizam, R.M., Ahmad-Fauzi, M.N., Mohamed, A.R. and Sreekantan, S., 2014. Effect of calcination temperature on the morphological and phase structure of hydrothermally synthesized copper ion doped TiO_2 nanotubes. *Advanced Materials Research*, 1024, pp.7-10.

[18] Ma, L., Fang, Z., Duan, J., Li, J., Zhu, K., Jiang, Y., Ji, B. and Yang, Z., 2024. Mesoporous TiO_2@ g-C_3N_4 nanostructure-enhanced photocatalytic degradation of tetracycline under full-spectrum sunlight. *Molecules*, 29(24), p.5981.

[19] Cao, X., Tao, J., Xiao, X. and Nan, J., 2018. Hydrothermal-assisted synthesis of the multi-element-doped TiO_2 micro/nanostructures and their photocatalytic reactivity for the degradation of tetracycline hydrochloride under the visible light irradiation. *Journal of Photochemistry and Photobiology A: Chemistry*, 364, pp.202-207.

[20] Romanovska, N., Manoryk, P., Selyshchev, O., Yaremov, P., Shylzshenko, O., Terebilenko, A., Shcherbakov, S. and Zahn, D.R.T., 2020. Influence of calcination temperature on structural-dimensional characteristics of C, S-doped TiO_2 nanostructures and their photocatalytic activity in the ceftazidime and doxycycline photodegradation processes. *Ukrainian Chemistry Journal*, 86, pp.95-119.

[21] Sangchay, W., 2013. Effect of calcinations temperature on the structural and photocatalytic activity of TiO_2 powders

prepared by sol-gel method. *Advanced Materials Research*, 626, pp.329-333.

[22] Mozia, S., 2008. Effect of calcination temperature on photocatalytic activity of TiO_2 Photodecomposition of mono-and polyazo dyes in water. *Polish Journal of Chemical Technology*, 10(3), pp.42-49.

[23] Yang, S., Ren, B., Chen, S., Liu, S., Zhang, Y. and Sun, Y., 2023. Influence of calcination temperature of TiO_2 nanowires via hydrothermal method for photocatalytic degradation. *Digest Journal of Nanomaterials and Biostructures*, 18, pp.47-54.

[24] Fan, J., Zhao, L., Yu, J. and Liu, G., 2012. The effect of calcination temperature on the microstructure and photocatalytic activity of TiO_2-based composite nanotubes prepared by an in situ template dissolution method. *Nanoscale*, 4(20), pp.6597-6603.

[25] Yang, J., Liu, Z., Wang, Y. and Tang, X., 2020. Construction of a rod-like Bi_2O_4 modified porous gC_3N_4 nanosheets heterojunction photocatalyst for the degradation of tetracycline. *New Journal of Chemistry*, 44(23), pp.9725-9735.

[26] Elbushra, H., Ahmed, M., Wardi, H. and Eassa, N., 2018. Synthesis and characterization of TiO_2 using sol-gel method at different annealing temperatures. *MRS Advances*, 3(42-43), pp.2527-2535.

[27] Han, J.Y. and Bark, C.W., 2014. Influence of calcination temperature on the structure and optical properties of $Bi_{3.25}La_{0.75}Ti_3O_{12}$ powders. *Journal of the Korean Physical Society*, 65, pp.216-221.

[28] Yihunie, M.T., 2023. Effect of temperature sintering on grain growth and optical properties of TiO_2 nanoparticles. *Journal of Nanomaterials*, 2023(1), p.3098452.

[29] Byrne, C., Fagan, R., Hinder, S., McCormack, D.E. and Pillai, S.C., 2016. New approach of modifying the anatase to rutile transition temperature in TiO_2 photocatalysts. *RSC advances*, 6, pp.95232-95238.

[30] Manikandan, K., JafarAhamed, A. and Brahmanandhan, G., 2017. Synthesis, structural and optical characterization of TiO_2 nanoparticles and its assessment to cytotoxicity activity. *Journal of Environmental Nanotechnology*, 6(3), pp.94-102.

[31] Mishra, V., Warshi, M.K., Sati, A., Kumar, A., Mishra, V., Kumar, R. and Sagdeo, P.R., 2019. Investigation of temperature-dependent optical properties of TiO_2 using diffuse reflectance spectroscopy. *SN Applied Sciences*, 1, p.241.

[32] Li, W., Liang, R., Hu, A., Huang, Z. and Zhou, Y.N., 2014. Generation of oxygen vacancies in visible light activated one-dimensional iodine TiO_2 photocatalysts. *RSC advances*, 4, pp.36959-36966.

[33] Qin, Y., Li, Y., Tian, Z., Wu, Y. and Cui, Y., 2016. Efficiently Visible-light driven photoelectrocatalytic oxidation of As (III) at low positive biasing using Pt/TiO_2 nanotube electrode. *Nanoscale research letters*, 11, p.32.

[34] Guo, Z., Prezhdo, O.V., Hou, T., Chen, X., Lee, S.T. and Li, Y., 2014. Fast energy relaxation by trap states decreases electron mobility in TiO_2 nanotubes: time-domain Ab initio analysis. *The Journal of Physical Chemistry Letters*, 5(10), pp.1642-1647.

[35] Souza, D.R., Neves, J.V.S., França, Y.K. and Malheiro, W.C., 2021. TiO_2 synthesis by the Pechini's method and application for diclofenac photodegradation. *Photochemistry and Photobiology*, 97(1), pp.32-39.

[36] Abbas, M., 2020. Experimental investigation of titanium dioxide as an adsorbent for removal of Congo red from aqueous solution, equilibrium and kinetics modeling. *Journal of Water Reuse and Desalination*, 10(3), pp.251-266.

[37] Parrino, F., De Pasquale, C. and Palmisano, L., 2019. Influence of surface-related phenomena on mechanism, selectivity, and conversion of TiO_2-induced photocatalytic reactions. *ChemSusChem*, 12(3), pp.589-602.

[38] Bouafia-Chergui, S., Zemmouri, H., Chabani, M. and Bensmaili, A., 2016. TiO_2-photocatalyzed degradation of tetracycline: kinetic study, adsorption isotherms, mineralization and toxicity reduction. *Desalination and Water Treatment*, 57(35), pp. 16670-16677.

[39] Galedari, M., Ghazi, M.M. and Mirmasoomi, S.R., 2019. Photocatalytic process for the tetracycline removal under visible light: Presenting a degradation model and optimization using response surface methodology (RSM). *Chemical Engineering Research and Design*, 145, pp.323-333.

[40] Li, W., Ding, H., Ji, H., Dai, W., Guo, J. and Du, G., 2018. Photocatalytic degradation of tetracycline hydrochloride via a CdS-TiO_2 heterostructure composite under visible light irradiation. *Nanomaterials*, 8(6), p.415.

[41] Phromma, S., Wutikhun, T., Kasamechonchung, P., Eksangsri, T. and Sapcharoenkun, C., 2020. Effect of calcination temperature on photocatalytic activity of synthesized TiO_2 nanoparticles via wet ball milling sol-gel method. *Applied Sciences*,10(3), p.993.

[42] Collins-Martínez, V., Ortiz, A.L. and Elguézabal, A.A., 2007. Influence of the anatase/rutile ratio on the TiO_2 photocatalytic activity for the photodegradation of light hydrocarbons. *International Journal of Chemical Reactor Engineering*, 5(1), p.92.

[43] Nasseh, N., Barikbin, B. and Taghavi, L., 2020. Photocatalytic degradation of tetracycline hydrochloride by $FeNi_3/SiO_2/CuS$ magnetic nanocomposite under simulated solar irradiation: Efficiency, stability, kinetic and pathway study. *Environmental Technology & Innovation*, 20, p.101035.

[44] Dona, J., Garriga, C., Arana, J., Pérez, J., Colon, G., Macías, M. and Navio, J.A., 2007. The effect of dosage on the photocatalytic degradation of organic pollutants. *Research on Chemical Intermediates*, 33, pp.351-358.

[45] Zhu, X., Wang, Y. and Zhou, D., 2014. TiO_2 photocatalytic degradation of tetracycline as affected by a series of environmental factors. *Journal of soils and sediments*, 14, pp.1350-1358.

[46] Zhenhai, W., Zikai, Z., Sen, W. and Zhi, F., 2024. Enhanced degradation of tetracycline by gas-liquid discharge plasma coupled with g-C_3N_4/TiO_2. *Plasma Science and Technology*, 26, p.094007.

[47] Zhang, J., Zhang, S., Bian, X., Yin, Y., Huang, W., Liu, C., Liang, X. and Li, F., 2024. High efficiency removal performance of tetracycline by magnetic $CoFe_2O_4/NaBiO_3$ photocatalytic synergistic persulfate technology. *Molecules*, 29(17), p.4055.

[48] Hasham Firooz, M., Naderi, A., Moradi, M. and Kalantary, R.R., 2024. Enhanced tetracycline degradation with

TiO_2/natural pyrite S-scheme photocatalyst. *Scientific Reports*, 14, p.4954.

[49] Oluwole, A.O. and Olatunji, O.S., 2022. Photocatalytic degradation of tetracycline in aqueous systems under visible light irridiation using needle-like SnO_2 nanoparticles anchored on exfoliated g-C_3N_4. *Environmental Sciences Europe*, 34, p.5.

[50] Hu, M., Chen, W. and Wang, J., 2024. Photocatalytic degradation of tetracycline by La-Fe Co-doped $SrTiO_3/TiO_2$ composites: performance and mechanism study. *Water*, 16(2), p.210.

[51] Zhu, K., Ma, L., Duan, J., Fang, Z. and Yang, Z., 2025. Photocatalytic degradation of tetracycline hydrochloride using TiO_2/CdS on nickel foam under visible light and RSM–BBD optimization. *Catalysts*, 15(2), p.113.

[52] Ma, Y., Peng, Q., Sun, M., Zuo, N., Mominou, N., Li, S., Jing, C. and Wang, L., 2022. Photocatalytic oxidation degradation of tetracycline over La/Co@ TiO_2 nanospheres under visible light. *Environmental Research*, 215(2), p.114297.

[53] Chen, X. and Mao, S.S., 2007. Titanium dioxide nanomaterials: synthesis, properties, modifications, and applications. *Chemical reviews*, 107(7), pp.2891-2959.

[54] Diebold, U., 2003. The surface science of titanium dioxide. *Surface science reports*, 48(5-8), pp.53-229.

[55] Nosaka, Y. and Nosaka, A.Y., 2017. Generation and detection of reactive oxygen species in photocatalysis. *Chemical reviews*, 117(17), pp.11302-11336.

[56] Scanlon, D.O., Dunnill, C.W., Buckeridge, J., Shevlin, S.A., Logsdail, A.J., Woodley, S.M., Catlow, C.R.A., Powell, M.J., Palgrave, R.G., Parkin, I.P., Watson, G.W., Keal, T.W., Sherwood, P., Walsh, A. and Sokol, A.A., 2013. Band alignment of rutile and anatase TiO_2. *Nature materials*, 12, pp.798-801.